torque rotates the projectile clockwise. On the rotated projectile with the c.m. at 3.4 cm from the tip, the torque is counterclockwise for either the type-b or type-c simulations and, therefore, tends to restore the projectile to its centered position. If the c.m. is at 7.4 cm, the torque is counterclockwise in the type-b simulation and clockwise in the type-c simulation. Therefore, the aerodynamic torque stabilizes the projectile if a normal shock is maintained on the rear part of the projectile and destabilizes the projectile if this shock is absent. On the projectile with the c.m. at 11.4 cm, the torque is clockwise for both types of simulations and, hence, destabilizes the projectile.

Conclusions

We have analyzed the stability of the projectile in the thermally choked ram accelerator based on the pressure information obtained from two-dimensional, reactive flow simulations. The analysis shows that the aerodynamic torque generated by the pressure imbalance because of a perturbation in the projectile position stabilizes the projectile if the c.m. of the projectile is near the projectile tip, and destabilizes the projectile if the c.m. is close to the projectile base. For the projectile with its c.m. located in the middle part of the projectile, similar to the projectile used in the experiments,[4] the aerodynamic torque stabilizes the projectile if a normal shock is maintained on the rear part of the projectile by the thermally choked combustion and destabilizes the projectile if this normal shock is absent. Since this thermally choked shock tends to stabilize the projectile, projectile canting could possibly be more serious in a failed launch process in which no thermally choked normal shocks are maintained on the rear part of the projectile. The normal shock generated by the thermally choked combustion is the key feature of the pressure distribution on the projectile and plays an important role in the projectile stability.

Acknowledgment

This work was supported by the U.S. Air Force Office of Scientific Research and the U.S. Naval Research Laboratory.

References

[1]Hertzberg, A., Bruckner, A. P., and Bogdanoff, D. W., "Ram Accelerator: A New Chemical Method for Accelerating Projectiles to Ultrahigh Velocities," *AIAA Journal*, Vol. 26, No. 2, 1988, pp. 195–203.

[2]Li, C., Kailasanath, K., and Oran, E. S., "Dynamics of Oblique Detonations in Ram Accelerators," *Shock Waves*, Vol. 5, No. 5, 1995, pp. 97–102.

[3]Li, C., Kailasanath, K., and Oran, E. S., "Detonation Structures on Ram-Accelerator Projectiles," AIAA Paper 94-0551, Jan. 1994.

[4]Bruckner, A. P., Knowlen, C., Hertzberg, A., and Bogdanoff, D. W., "Operational Characteristics of the Thermally Choked Ram Accelerator," *Journal of Propulsion and Power*, Vol. 7, No. 1, 1991, pp. 15–26.

[5]Li, C., Kailasanath, K., and Oran, E. S., "Analysis of Transient Flows in Thermally Choked Ram Accelerator," AIAA Paper 93-2187, June 1993.

[6]Boris, J. P., and Book, D. L., "Solution of the Continuity Equations by the Method of Flux-Corrected Transport," *Methods of Computational Physics*, Vol. 16, No. 1, 1976, pp. 85–107.

[7]Oran, E. S., Boris, J. P., Young, T., Flanigan, M., Burk, T., and Picone, M., "Numerical Simulations of Detonations in Hydrogen-Air and Methane-Air Mixtures," *Proceedings of the 18th International Symposium on Combustion*, Vol. 18, The Combustion Inst., Pittsburgh, PA, 1981, pp. 1641–1649.

[8]Landsberg, A. M., Young, T. R., and Boris, J. P., "An Efficient, Parallel Method for Solving Flows in Complex Three-Dimensional Geometries," AIAA Paper 94-0413, Jan. 1994.

[9]Li, C., Kailasanath, K., and Oran, E. S., "Detonation Structures Behind Oblique Shocks," *Physics of Fluids*, Vol. 6, No. 4, 1994, pp. 1600–1605.

[10]Li, C., Kailasanath, K., and Oran, E. S., "Analysis of Stability of Projectiles in Thermally Chocked Ram Accelerators," AIAA Paper 96-0344, Jan. 1996.

Modified Spalart–Allmaras One-Equation Turbulence Model for Rough Wall Boundary Layers

Jaesoo Lee* and Gerald C. Paynter†
Boeing Commercial Airplane Group,
Seattle, Washington 98124-2207

Nomenclature

A = constant (=26.0) in van Driest's damping function
k = roughness height
k_s = equivalent sand–grain roughness height
k_s^+ = roughness Reynolds number, $k_s u_\tau/\nu$
u, v = velocity components in the streamwise and the normal to surface direction
u_τ = frictional velocity
x, y = coordinates in the streamwise and the normal to boundary-layer surface directions
θ = momentum thickness
$\varkappa$ = von Kármán constant, 0.41
ν = kinematic molecular viscosity
ν_t = kinematic eddy viscosity

Superscript
$+$ = quantity normalized by ν/u_τ

Introduction

Acoustic lining materials are widely used in inlets and exhaust nozzles to reduce engine noise. These acoustically treated surfaces are aerodynamically rough and cause the turbulent boundary layer to thicken more rapidly than for a smooth surface. Separation locations, the size of the separation bubbles, and the performance of inlets and nozzles all change with roughness. Including surface roughness effects in computational fluid dynamics simulation of fluid flows is, therefore, necessary to improve the accuracy of aerodynamic performance prediction for inlets and nozzles, etc.

The roughness effect on the boundary-layer velocity profile can be accounted for by modifying the eddy dissipation near rough wall surface as suggested by Rotta.[1] Rotta interpreted surface roughness as a reduction of the viscous sublayer. He suggested that the universal law of the wall applies when the plane of reference is shifted in the coordinate direction toward the wall by a small distance R as illustrated in Fig. 1.

Based on the Rotta concept,[1] Cebeci and Chang (C–C) (Ref. 2) developed a roughness model by modifying the inner model of Cebeci and Smith's algebraic turbulence model to include the surface roughness effect. They shifted the reference coordinate system by R toward the wall and calculated the eddy viscosity based on the effective distance from wall, $y + R$:

$$\nu_t = \varkappa^2 (y + R)^2 \left[1 - \exp\frac{-(y + R)^+}{A^+}\right]^2 \left|\frac{du}{dy}\right| \tag{1}$$

where a shift from the wall surface R is a function of k_s^+ and the boundary-layer properties, and was written as

$$R = (0.9\nu/u_\tau)[\sqrt{k_s^+} - k_s^+ \exp(-k_s^+/6)] \tag{2}$$

Presented as Paper 95-7087 at the 12th ISABE in Melbourne, Australia, Sept. 10–15, 1995; received Oct. 9, 1995; revision received Feb. 12, 1996; accepted for publication Feb. 22, 1996.

*Principal Engineer, Propulsion Research CFD, M/S 49-53. Member AIAA.

†Propulsion Research CFD, M/S 49-53. Associate Fellow AIAA.

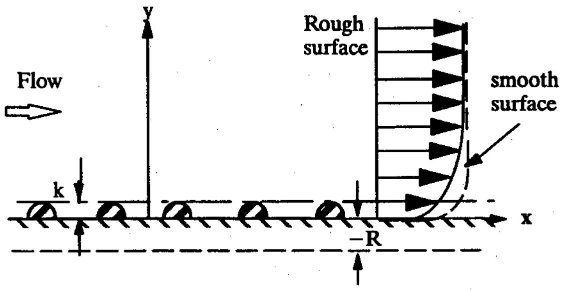

Fig. 1 Boundary-layer thickening on a rough surface and a reference coordinates system (x–y).

Equation (1) implies that the eddy viscosity on a rough wall is nonzero and increases with the modified mixing length $y + R$, which results in a reduction of the viscous sublayer. The C–C model was evaluated using a parabolic marching code for two-dimensional turbulent boundary-layer flows[3] and a Navier–Stokes code, PARC (Ref. 4). The model works well in predicting turbulent boundary-layer flows over acoustically treated rough surfaces when there is no flow separation.[2,5,6] However, to predict separated boundary-layer flows in three dimension and installed inlet and nozzle flows, a roughness model based on a transport equation-type turbulence model is needed.

The objective of the present study was to develop a transport equation-type turbulence model for boundary-layer flows over rough surfaces by modifying the Spalart–Allmaras (S–A) one-equation turbulence model.[7]

Approach

The S–A turbulence model was shifted by a distance R toward the wall using a similar coordinate transformation to that for the C–C model. The model equation was also simplified to implement into a two-dimensional, parabolized, steady-state boundary-layer analysis code[4] as

$$u\frac{\partial\tilde{\nu}}{\partial x} + v\frac{\partial\tilde{\nu}}{\partial y} = \frac{1}{\sigma}\left[\frac{1}{\partial y}(\nu + \tilde{\nu})\frac{\partial\tilde{\nu}}{\partial y}\right] + c_{b1}\tilde{S}\tilde{\nu} + \frac{c_{b2}}{\sigma}\left(\frac{\partial\tilde{\nu}}{\partial y}\right)^2 - c_{w1}f_w\left(\frac{\tilde{\nu}}{d+R}\right)^2 \tag{3}$$

where

$$\tilde{S} = S + \frac{\tilde{\nu}}{\varkappa^2(d+R)^2}f_{v2}, \qquad f_w = g\left(\frac{1 + c_{w3}^6}{g^6 + c_{w3}^6}\right)^{1/6}$$

$$f_{v2} = 1 - \frac{\chi}{1 + \chi f_{v1}}, \quad g = r + c_{w2}(r^6 - r)$$

$$r = \frac{\tilde{\nu}}{S\varkappa^2(d+R)^2}$$

Here, S is the magnitude of vorticity and d is the distance from the surface. R is defined by Eq. (1). Note that the coordinate transformation changed the production and destruction terms and the coefficients of the S–A model. The kinematic eddy viscosity is obtained using

$$\nu_t = \tilde{\nu}f_{v1} \tag{4}$$

where

$$f_{v1} = \frac{\chi^3}{\chi^3 + c_{v1}^3} \quad \text{and} \quad \chi = \frac{\tilde{\nu}}{\nu}$$

The empirical constants, c_{b1}, c_{b2}, σ, c_{w1}, c_{w2}, c_{w3}, c_{v1}, and $\varkappa$ are the same as the values used in the original S–A model.

The boundary condition on rough surface was estimated by setting $y = 0$ in Eq. (1):

$$\nu_t|_{y=0} = \varkappa^2R^2\left(1 - \exp - \frac{R^+}{A^+}\right)^2\left|\frac{du}{dy}\right| \tag{5}$$

The eddy viscosity profile at the starting location was initialized using the C–C turbulence model based on the incoming velocity profile. The velocity profile at the starting location was estimated by Cole's compressible law of the wall and wake formula using the experimental momentum thickness and shape factor.

Equation (3) was discretized using an upwind differencing scheme combined with linearization of the source terms to adapt to the boundary-layer analysis code. The resulting tridiagonal matrix (TDM) form of Eq. (3) was solved using a TDM solution algorithm, decoupled from the solution of the boundary-layer equations. The modified S–A model usually converged to a satisfactory solution within two inner iterations. The first grid spacing parallel to the rough surface was refined to maintain the y^+ value on the order of 0.5.

The equivalent sand–grain roughness heights for the rough surfaces considered in the present study were the same values used by Cebeci and Chang.[2] In general, a k_s for a rough surface can be determined using a two-dimensional boundary-layer method by varying k_s input until the predicted momentum thickness growth matches that which was obtained experimentally. The growth of momentum thickness is considered because it is closely related with the pressure loss because of surface roughness.

Results and Discussion

The modified S–A turbulence model was evaluated using experimental momentum thickness growth data for the boundary-layer development over acoustically treated surfaces.[8–11] The growth of measured momentum thickness was compared with those predicted using the C–C and the modified S–A model.

Figure 2 shows typical velocity profiles plotted on a semilogarithmic inner coordinate system that were predicted using the modified S–A model. It clearly shows the reduction of viscous sublayer and the downshift of the velocity profiles due to roughness which is consistent with the experimental data.

Figure 3 shows the comparisons of measured momentum thickness growths and predicted results using the C–C and the

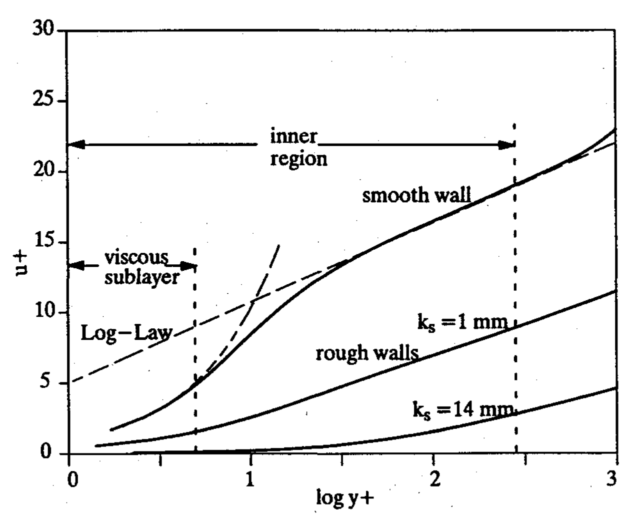

Fig. 2 Downshift of near-wall velocity profile from surface roughness effect.

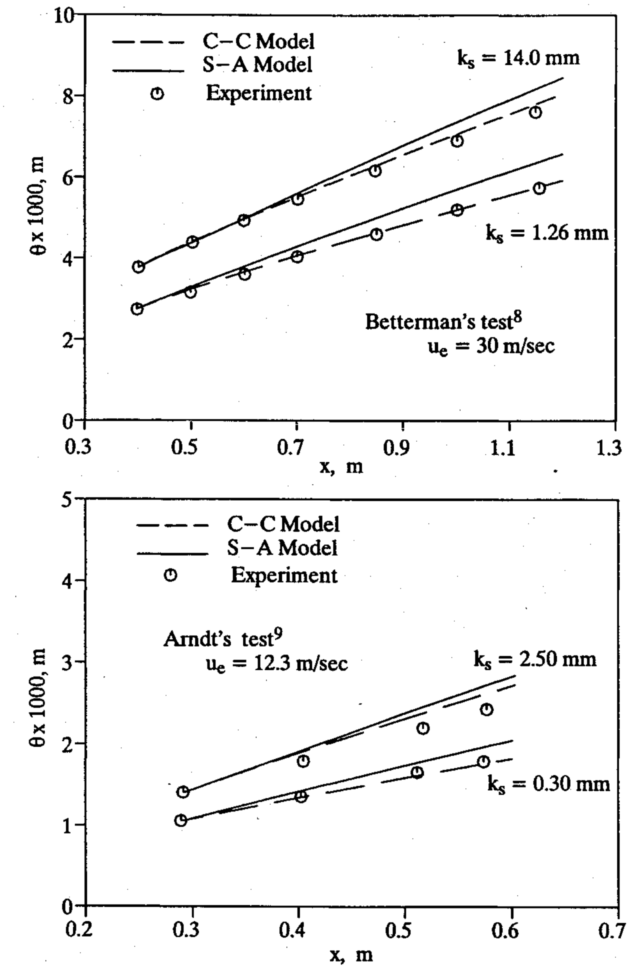

Fig. 3 Comparison of predicted and measured momentum thicknesses for boundary-layer flows under zero pressure gradient.

modified S–A models for Betterman's and Arndt et al.'s tests. For both comparisons shown, surface roughness conditions were varied by two levels at a fixed freestream velocity of 30 m/s. The predicted results using the modified S–A model are in good agreement with the measured data over a distance of approximately 1 m. However, Fig. 3 shows that the C–C model predicts the momentum thickness growth more accurately than the S–A model at the k_s values used. The slight overprediction tendency with the S–A model is partly because of the fundamental difference between the two turbulence models. Another reason could be that the k_s values reported by Cebeci and Chang[2] might be slightly higher than for the modified S–A model. No attempt was made in the present study to obtain the best agreement by slightly lowering k_s values for the modified S–A model.

The effect of pressure gradient on the boundary-layer development on rough surfaces was examined using Coleman et al.[10] and Scottron et al.[11] tests for favorable and adverse pressure gradient conditions, respectively. Their tests were conducted at two different levels of pressure gradient while keeping the freestream velocity and surface roughness conditions the same. Predicted and measured results are compared in Fig. 4. The predicted momentum thickness growth for both the C–C and the S–A models are in good agreement with the experimental data except that both the C–C and the modified S–A models overpredicted the experimental results for the strong adverse pressure gradient case. This overprediction with strong adverse pressure gradient may be attributed to the limited capability of the parabolic boundary-layer analysis method that was used in the present study.

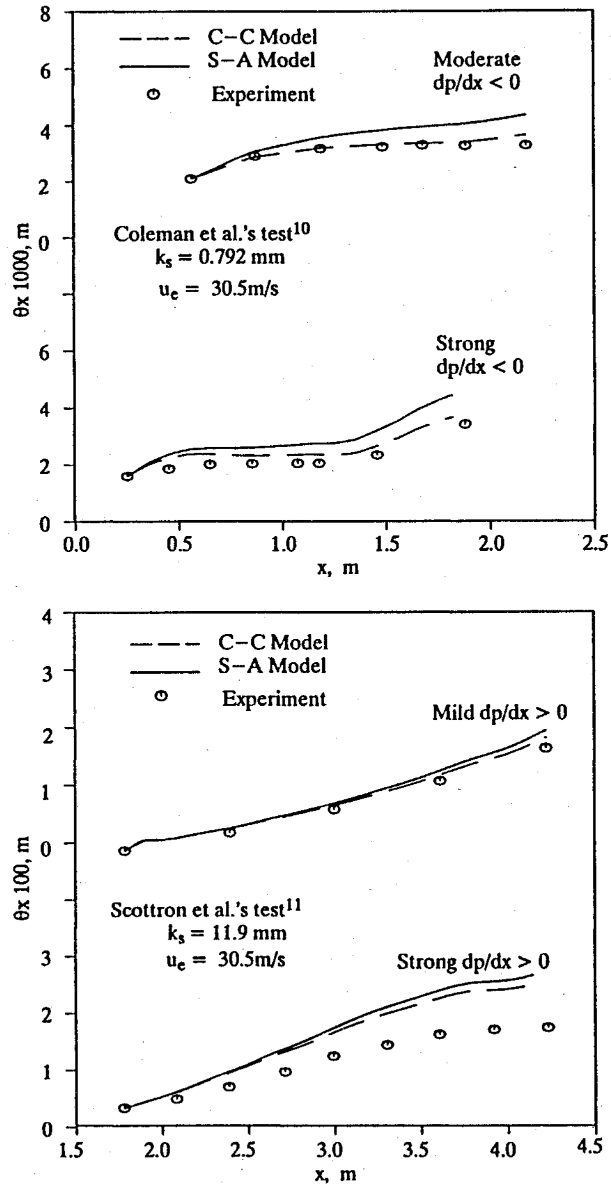

Fig. 4 Comparison of predicted and measured momentum thicknesses for boundary-layer flows under favorable and adverse pressure gradients.

Conclusions

A turbulence model for boundary-layer flows over rough surfaces has been developed by modifying the S–A one-equation turbulence model. The model was evaluated against experimental data for flows developing over acoustically treated rough surfaces with different surface roughness, freestream velocity, and pressure gradient conditions. The modified S–A turbulence model was demonstrated by predicting boundary-layer flows over rough surfaces. The developed modeling approach based on a transport-type turbulence model should enable the three-dimensional Navier–Stokes analysis of inlets and nozzles to include roughness effects for more accurate performance predictions.

References

[1]Rotta, J. C., "Turbulent Boundary Layers in Incompressible Flow," *Progress in Aerospace Science*, Vol. 2, 1962, pp. 1–219.

[2]Cebeci, T., and Chang, K. C., "Calculation of Incompressible Rough Wall Boundary Layer Flows," *AIAA Journal*, Vol. 16, No. 7, 1978, pp. 730–735.

[3]Reyhner, T. A., "Finite Difference Solution of the Compressible Turbulent Boundary Layer Equations," *Proceedings of Computation*

of Turbulent Boundary Layers—1968 AFOSR—IFP—Stanford Conference, Vol. 1, Stanford Univ., Stanford, CA, pp. 375–383.

[4]Cooper, G. K., "The PARC Code: Theory and Usage," Arnold Engineering and Development Center, TR-87-24, Oct. 1987.

[5]Lee, J., Sloan, M. L., and Paynter, G. C., "A Lag Model for Turbulent Boundary Layers Developing over Rough Bleed Surfaces," AIAA Paper 93-2988, July 1993.

[6]Paynter, G. C., Treiber, D. A., and Kneeling, W. D., "Modeling Supersonic Inlet Boundary Layer Bleed Roughness," *Journal of Propulsion and Power*, Vol. 9, No. 4, 1993, pp. 622–627.

[7]Spalart, P. R., and Allmaras, S. R., "A One-Equation Turbulence Model for Aerodynamic Flows," AIAA Paper 92-0439, Jan. 1992.

[8]Betterman, D., "Contribution a l'Etude de la Couche Limite Turbulente le Long de la Plaques Rugueuses," Centre National de la Recherche Scientifique, Rept. 65-6, Paris, 1965.

[9]Arndt, R. E. A., and Ippen, A. T., "Cavitation near Surfaces of Distributed Roughness," Hydrodynamics Lab., Dept. of Civil Engineering, Massachusetts Inst. of Technology, Rept. 104, Cambridge, MA, 1967.

[10]Coleman, H. W., Moffat, R. J., and Kays, W. M., "Momentum and Energy Transport in the Accelerated Fully Rough Turbulent Boundary Layer," Dept. of Mechanical Engineering, Stanford Univ., Rept. HMT-24, Stanford, CA, 1976.

[11]Scottron, V. E., and Power, J. L., "The Influence of Pressure Gradient on the Turbulent Boundary Layer over a Rough Surface," Navy Dept., David Taylor Model Basin, Washington, DC, Rept. 2115, 1965.

Boundary-Layer Tripping by a Roughness Element

Jamal A. Masad*
High Technology Corporation,
Hampton, Virginia 23666

Introduction

BOUNDARY-LAYER tripping is desired in scramjet as well as heat-exchanger design to enhance, respectively, mixing and heat transfer rates. Furthermore, the achievement of earlier transition by artificial tripping of the boundary layer is often desired in wind-tunnel operations to simulate turbulent boundary-layer behavior at full-scale Reynolds numbers. The most common method for tripping the boundary layer is the use of roughness. The existence of roughness enhances the instability of the flow and accelerates the onset of transition and, consequently, the occurrence of turbulence. It is known that tripping the boundary layer with roughness elements becomes more difficult at higher speeds. This was first evident because large-diameter wires were needed to trip the boundary layer at high speeds.

The occurrence of laminar separation on aerodynamic surfaces increases pressure drag that results in a reduction in the efficiency of these surfaces. Separation can result from a localized adverse pressure gradient created by surface roughness, or it can result from extended regions of adverse pressure gradient because of the curvature of the surface. In both cases, the flow may separate while it is still laminar.[1] In situations in which laminar separation is about to occur, tripping the boundary layer so that it remains attached is preferable. Transition causes the point of separation to move downstream because in a turbulent boundary layer the accelerating influence of the external flow extends farther because of turbulent mixing. This in turn, reduces the pressure drag.

The critical tripping height of a roughness element is defined as the minimum height that causes transition at the downstream end of the roughness element. In this work, we quantify the variation of the critical tripping height of a roughness element with parameters such as the freestream Mach and Reynolds numbers and the length of the roughness element. Our approach consists of using linear stability theory, coupled with the empirical e^N method, to predict the transition onset location.

The presence of a roughness element on a surface can produce a separation bubble behind it if and when its height becomes sufficiently large. In such flows, both a strong viscous–inviscid interaction and an upstream influence are known to exist. The conventional boundary-layer formulation fails to predict such flows; therefore, one needs to use a triple-deck theory, an interacting boundary layer (IBL) theory,[2] or a Navier–Stokes solver to analyze them. In this work we use the IBL theory to predict such flows.

The numerical results presented in this work are for two-dimensional compressible subsonic flow over a single, smooth, two-dimensional hump on a flat plate. The results are for a two-parameter family of symmetric hump shapes given by

$$y = y^*/L^* = (k^*/L^*)f(z) = kf(z) \tag{1}$$

where

$$z = 2(x^* - L^*)/\lambda^* = 2(x - 1)/\lambda \tag{2}$$

$$f(z) = \begin{cases} 1 - 3z^2 + 2|z|^3, & \text{if } |z| \le 1 \\ 0, & \text{if } |z > 1| \end{cases} \tag{3}$$

Here, k^* is the dimensional height of the symmetric hump; it is positive for a hump and negative for a dip. The parameter λ^* is the dimensional length of the hump with the center located at $x^* = L^*$.

For stability analysis, we use spatial quasiparallel instability. By solving the linear instability eigenvalue problem, we obtain the disturbance-wave growth rate as a function of location on the flat surface. The transition onset location is then empirically correlated with the location at which the integrated growth rate (N factor) of the disturbance wave reaches a certain value. This is the empirical N-factor transition criterion (i.e., the criterion that utilizes the e^N method) proposed by Smith and Gamberoni[3] based on experimental data (see also Jaffe et al.[4]). For flow over a flat plate, transition was found to occur when the N factor reached a value close to 9. We denote the value of Re_x at which the N factor reaches a value of 9 by $(Re_x)_{N=9}$.

The length of a roughness element influences considerably the predicted transition onset location.[5] However, the effect of the length of a roughness element on flow instability and transition location is usually overlooked in the literature. Although the experimental correlations of Fage[6] and Carmichael[7] account for the effect of roughness length on transition location, the commonly used Re_k correlation does not.

The role of the hump length is opposite that of the hump height. If the nondimensional length $\lambda = \lambda^*/L^*$ of a hump at a fixed height is decreased, then the location where the N factor first reaches a value of 9 is shifted upstream. When the roughness element becomes so short that its length falls below a certain critical value, the upstream movement of the transition location slows down considerably, and the predicted transition location approaches the downstream end of the roughness element.

Variation of the nondimensional critical tripping height k_{crit} with the nondimensional length of the hump λ is shown in Fig. 1. The results are for incompressible flow at a freestream

Received Sept. 23, 1995; revision received Feb. 14, 1996; accepted for publication Feb. 22, 1996.

*Research Scientist, 28 Research Drive, P.O. Box 7262. Senior Member AIAA.